

Nonlinear wave propagation in dense vapor of Bethe-Zel'dovich-Thompson fluids subjected to temperature gradients

Chandrasekaran, N. B.; Mercier, B.; Colonna, P.

DOI

[10.1063/5.0063226](https://doi.org/10.1063/5.0063226)

Publication date

2021

Document Version

Final published version

Published in

Physics of Fluids

Citation (APA)

Chandrasekaran, N. B., Mercier, B., & Colonna, P. (2021). Nonlinear wave propagation in dense vapor of Bethe-Zel'dovich-Thompson fluids subjected to temperature gradients. *Physics of Fluids*, 33(10), Article 107109. <https://doi.org/10.1063/5.0063226>

Important note

To cite this publication, please use the final published version (if applicable). Please check the document version above.

Copyright

Other than for strictly personal use, it is not permitted to download, forward or distribute the text or part of it, without the consent of the author(s) and/or copyright holder(s), unless the work is under an open content license such as Creative Commons.

Takedown policy

Please contact us and provide details if you believe this document breaches copyrights. We will remove access to the work immediately and investigate your claim.

Nonlinear wave propagation in dense vapor of Bethe–Zel'dovich–Thompson fluids subjected to temperature gradients

Cite as: Phys. Fluids **33**, 107109 (2021); <https://doi.org/10.1063/5.0063226>

Submitted: 13 July 2021 • Accepted: 23 September 2021 • Published Online: 12 October 2021

 N. B. Chandrasekaran,  B. Mercier and  P. Colonna



View Online



Export Citation



CrossMark

ARTICLES YOU MAY BE INTERESTED IN

[Effect of co-flow on fluid dynamics of a cough jet with implications in spread of COVID-19](#)
Physics of Fluids **33**, 101701 (2021); <https://doi.org/10.1063/5.0064104>

[On the relationships between different vortex identification methods based on local trace criterion](#)
Physics of Fluids **33**, 105116 (2021); <https://doi.org/10.1063/5.0063326>

[Wall-attached structures over a traveling wavy boundary: Scalar transport](#)
Physics of Fluids **33**, 105115 (2021); <https://doi.org/10.1063/5.0065449>

LEARN MORE

 Author Services

Maximize your publication potential with
English language editing and
translation services



Nonlinear wave propagation in dense vapor of Bethe–Zel’dovich–Thompson fluids subjected to temperature gradients

Cite as: Phys. Fluids **33**, 107109 (2021); doi: 10.1063/5.0063226

Submitted: 13 July 2021 · Accepted: 23 September 2021 ·

Published Online: 12 October 2021



View Online



Export Citation



CrossMark

N. B. Chandrasekaran,^{a)} B. Mercier,^{b)} and P. Colonna^{c)}

AFFILIATIONS

Propulsion and Power, Delft University of Technology, 2629HS, Delft, the Netherlands

^{a)}Electronic mail: n.b.chandrasekaran@tudelft.nl

^{b)}Electronic mail: b.h.mercier@tudelft.nl

^{c)}Author to whom correspondence should be addressed: p.colonna@tudelft.nl

ABSTRACT

Flows of fluids made of complex organic molecules exhibit unconventional fluid dynamic behavior in the vapor phase if their thermodynamic state is close to that of the vapor–liquid critical point. If the molecule is sufficiently complex, this thermodynamic domain is characterized by negative values of the fundamental derivative of gasdynamics Γ , the fluid is called Bethe–Zel’dovich–Thompson (BZT) fluid, and atypical phenomena, such as rarefaction shockwaves, are theoretically admissible. The nature of the steepening of nonlinear waves in dense vapor flows of organic fluids evolving in this thermodynamic region can be significantly affected by the presence of temperature gradients in the flow. This study investigates the evolution of finite-amplitude acoustic waves in these conditions. The steepening of the wavefront is analyzed using the wavefront expansion technique, and the deformation of the wavefront is simulated numerically by solving the Westervelt equation. The results of simulations of wave propagation in dense vapors indicate that, though Γ governs the nature of steepening waves, local gradients in sound speed and density can alter the rate of steepening and can enhance or delay shock formation in the medium, a result relevant also to the envisaged experiments aimed at proving the existence of nonclassical gasdynamics phenomena in BZT vapors.

© 2021 Author(s). All article content, except where otherwise noted, is licensed under a Creative Commons Attribution (CC BY) license (<http://creativecommons.org/licenses/by/4.0/>). <https://doi.org/10.1063/5.0063226>

I. INTRODUCTION

The thermodynamic states of a fluid with temperatures and pressures close to the values at the vapor–liquid critical point form a region characterized by changing values of the fundamental derivative of gasdynamics Γ , defined as

$$\Gamma \equiv 1 + \frac{\rho}{c} \left(\frac{\partial c}{\partial \rho} \right)_s, \quad (1)$$

where ρ is the density, c is the sound speed, and s is the entropy. As the name suggests, Γ is therefore inherently related to the way a wave propagates in fluids.^{1,2} In the case of ideal gases, Γ is greater than 1 and equal to $(\gamma + 1)/2$ where $\gamma = c_p/c_v$ is the ratio of specific heats. It has been shown that, for organic fluids made by large and complex molecules, Γ may have a value lower than 1 and may even become negative at thermodynamic conditions close to those of the critical point of the fluid. This set of thermodynamic states characterized by

negative values of the fundamental derivative is referred to in gasdynamics as the *nonclassical thermodynamic region*. Flows in which the fluid thermodynamic states are characterized by $\Gamma < 1$ are said to be in the non-ideal compressible fluid dynamic (NICFD) regime. Fluids featuring thermodynamic states for which $\Gamma < 0$ are known collectively as Bethe–Zel’dovich–Thompson (BZT) fluids.³ Unconventional gasdynamic phenomena, such as rarefaction shockwaves, which cannot be observed in classical flows because they violate fundamental principles, are instead theoretically admissible in flows of BZT fluids and for the stated thermodynamic conditions.⁴

The existence of a thermodynamic region with negative nonlinearity and the formation of rarefaction shock waves (RSW) have been extensively studied from a theoretical point of view, but the few experimental attempts to prove the actuality of nonclassical gasdynamics have led to inconclusive results so far. The first attempt to experimentally verify the formation of RSWs was carried out by Borisov *et al.*⁵ using Freon-13 (trichlorouromethane, CClF₃) as the test fluid. They

claimed to have observed a RSW in the vapor region close to its critical point. However, this result has been confuted by many authors citing the impossibility for Γ to be negative for vapor states of Freon-13, as the molecule is insufficiently complex. Therefore, the possibility that the measured flow was affected by so-called critical point phenomena and two-phase effects is minimal.⁶ A second shock-tube experiment aimed at generating and measuring RSW was conducted at the University of Colorado at Boulder using perfluorofluorene (PP10, C₁₃F₂₂) as the working fluid.⁷ However, no meaningful experimental result was achieved due to the thermal degradation of PP10 at the high operating temperatures. This was possibly due to the presence of air and moisture within the working fluid, which are known catalysts for thermochemical decomposition.^{8,9} The flexible asymmetric shock tube (FAST) at Delft University of Technology is one such facility designed with the intent of providing the experimental evidence for the formation of rarefaction shocks and therefore for the existence of nonclassical gasdynamic regime.^{9,10} Dodecamethylcyclohexasiloxane (D₆) was chosen as the test fluid, given its high level of thermal stability, non-toxicity, low level of flammability, and comparatively better accuracy of thermodynamic models.^{11,12} All these experiments were based on the assumption of homogeneous thermodynamic conditions of the vapor along the shock tube. Mathijssen *et al.*⁹ performed preliminary experiments in the FAST on the propagation of rarefaction waves in the non-ideal regime of siloxane D₆ at temperatures up to 300 °C and estimated values of the wave speed and sound speed that were within 8% and 1.6% of the predictions of a state-of-the-art thermodynamic model. Recent repeated temperature measurements performed by the authors of this article along the inner surface of the high-pressure tube of the FAST setup have shown that, even with the numerous precautions and tight control adopted to ensure the uniform temperature of the fluid, the vapor is always subjected to gradients in temperature in the longitudinal direction. Apart from the general interest in extending the acoustic theory to BZT fluids, thus to wave propagation in nonclassical flow conditions, it is therefore of interest to investigate the effect of such temperature variations on the formation of shock waves in these fluids in order to improve the interpretation of envisaged experiments.

The propagation of waves in fluids affected by non-uniform temperature distribution has been investigated by several authors. Soukhomlinov *et al.*¹³ studied the propagation of a weak shockwave in ideal gases with mild temperature gradients. They established an analytical solution to the one-dimensional wave propagation equation and compared the results with those obtained by numerically solving the Euler flow equation. Lin and Szeri¹⁴ investigated the effect of entropy gradients on shock formation in ideal gases using the wavefront expansion technique. They developed an analytical criterion for computing the shock formation distance and time, for a finite-amplitude wave traveling in a medium with smoothly varying entropy. However, the ideal gas assumption at the basis of these studies is no longer valid if the thermodynamic states of the vapor are close to the vapor-liquid critical state. A more general analysis was presented by Cramer and Kluck¹⁵ the scientists developed a weak shock theory for one-dimensional small-amplitude waves propagating in inviscid flows, by considering also cases in which the fundamental derivative associated with fluid states in the flow changes sign. Cramer and Sen¹⁶ extended this study by investigating the steepening of one-dimensional finite-amplitude waves in van der Waal vapors featuring

an embedded thermodynamic region of negative nonlinearity. An analytical solution for the steepening of a wavefront propagating in a medium with both positive and negative nonlinearities based on the wavefront expansion technique is presented by Muralidharan and Sujith.¹⁷ Though the solution is valid for any equation of state (EoS), the authors limit their study to a van der Waal's gas in the near-critical thermodynamic region. An alternate approach based on the Rubin–Rosenau–Gottlieb theory for the study of finite-amplitude wave propagation in thermoviscous fluids is described by Jordan *et al.*¹⁸

In the study documented here, the analytical solution obtained with the so-called wavefront expansion technique was employed to investigate the propagation of finite-amplitude waves in BZT fluids with axial temperature variations. This investigation is motivated by observations made by the authors while trying to improve the FAST⁹ that in any shock tube setup developed to study RSWs, temperature gradients along the tube are inevitable. Moreover, in this study multi-parameter equation of state was employed to model fluid properties¹⁹ in order to achieve the highest accuracy. The validity of the inviscid analysis is tested against viscous effects by comparing with the solution of the one-dimensional Westervelt equation. In addition, the effects of such gradients on shock formation distances were also computed. This paper is structured as follows: in Secs. II A and II B, the Westervelt equation and the numerical method used to solve the equation are introduced. This is followed by a brief description of the analytical solution in Sec. II C. Sections III A 1 and III A 2 treat the steepening characteristics of waves in case the thermodynamic state of the fluid is close to the $\Gamma = 0$ condition. The discussion is followed by a comparison between the analytical solution of the propagation equation with the results of the solution of the Westervelt equation (Sec. III A 3). Section III B discusses the effect of temperature gradients on shock formation distances in BZT fluids. Concluding remarks are summarized in Sec. IV.

II. METHODOLOGY

A. Westervelt Equation

The Westervelt equation is a well-known mathematical model in nonlinear acoustics that is widely adopted in studies concerning several industrial and medical applications including diagnostic ultrasound, sonochemistry, etc.^{20,21} Assuming that the disturbances in the fluid properties are of small amplitude relative to the medium at rest, and that the wave propagates in a fluid in which the length scale of the inhomogeneity is larger than the wavelength of the wave, the propagation of finite amplitude disturbances in a thermoviscous fluid can be written as^{22,23}

$$\nabla^2 p - \frac{1}{c_0^2} \frac{\partial^2 p}{\partial t^2} - \frac{1}{\rho_0} \nabla \rho_0 \nabla p + \frac{\delta}{c_0^4} \frac{\partial^3 p}{\partial t^3} + \frac{\Gamma}{\rho_0 c_0^4} \frac{\partial^2 p^2}{\partial t^2} = 0, \quad (2)$$

where p is the acoustic pressure, c_0 and ρ_0 are the sound speed and density of the quiescent fluid, δ is the diffusivity of sound, and Γ is the fundamental derivative of gasdynamics. The first two terms of Eq. (2) makeup the 1D linear wave equation describing the linear and lossless wave propagation at the small-signal sound speed. The third term accounts for the variation in density, and the fourth term for the losses due to thermal and viscous effects. The fifth term in Eq. (2) models the nonlinear distortion of the wave arising from finite amplitude effects.

In nonlinear acoustics, the fluid thermodynamic property associated with the variation of the sound speed is termed the *coefficient of nonlinearity* β and is defined as²⁴

$$\beta \equiv 1 + \frac{B}{2A}, \quad (3)$$

where A and B are the first and second order coefficients in the pressure-explicit virial equation of state of the fluid written as a function of density at constant entropy.^{24,25} Their ratio, B/A , is called *nonlinearity parameter*. It can easily be shown by using basic thermodynamic relations that β and Γ , the fundamental derivative of gasdynamics, are the same thermodynamic property called in different ways. Since the gaseous fluids dealt with in acoustics are treated under the ideal gas assumption, β , and hence Γ , in conventional acoustics is positive and larger than 1. However, if acoustic phenomena occur in the so-called non-ideal compressible fluid dynamics (NICFD) regime, thus close to vapor saturation and for high values of the reduced pressure P_r and the reduced temperature T_r , Γ is lower than 1. The value of Γ can even be lower than zero for some thermodynamic states if the medium is a BZT fluid, and in these conditions, the speed of sound decreases with density at constant entropy.

B. Solution of the Westervelt equation

The Westervelt equation does not have a known analytical solution and is, therefore, solved using numerical methods. Spatial and temporal derivatives in Eq. (2) are approximated with discrete differences using the finite difference time domain (FDTD) method.²⁶ The x spatial dimension is divided into N_x elements, equally spaced by Δx and indexed with i . Absorbing boundary conditions are imposed to prevent wave reflections that are numerical artifacts from affecting the results. The spatial derivative is computed using second-order-accurate central differences as

$$\frac{\partial p}{\partial x} \approx \frac{1}{2\Delta x} (p_i^{n+1} - p_i^{n-1}) \quad (4a)$$

$$\frac{\partial^2 p}{\partial x^2} \approx \frac{1}{\Delta x^2} (p_{i+1}^n - 2p_i^n + p_{i-1}^n). \quad (4b)$$

Similarly, the temporal dimension is discretized into N_t elements, divided into equal intervals Δt and indexed with n . The time derivative in the second term of Eq. (2) is computed using second-order-accurate central differences while the nonlinear and absorption terms are expanded using backward differencing, resulting in

$$\frac{\partial^2 p}{\partial t^2} \approx \frac{1}{(\Delta t)^2} (p_i^{n+1} - 2p_i^n + p_i^{n-1}) \quad (5a)$$

$$\frac{\partial^3 p}{\partial t^3} \approx \frac{1}{(2\Delta t)^3} (5p_i^n - 18p_i^{n-1} + 24p_i^{n-2} - 14p_i^{n-3} + 3p_i^{n-4}), \quad (5b)$$

$$\frac{\partial^2 p^2}{\partial t^2} \approx 2 \left[\left(\frac{3p_i^n - 4p_i^{n-1} + p_i^{n-2}}{2\Delta t} \right)^2 + \frac{2p_i^n - 5p_i^{n-1} + 4p_i^{n-2} - p_i^{n-3}}{\Delta t^2} \right]. \quad (5c)$$

Equations (4) and (5) are substituted into Eq. (2) and solved for p_i^{n+1} .

C. Method for the simulation of the wavefront propagation—wavefront expansion technique

If a finite-amplitude rarefaction wave travels in a homogeneous medium featuring a thermodynamic state with negative Γ , accepted theory prescribes that it steepens as a result of the nonlinearity. Given sufficient amplitude of the initial disturbance, the steepening of the wave can eventually result in the formation of a rarefaction shockwave (RSW). Numerically, the formation of a RSW can be identified by tracking the rate of steepening of the leading edge of the disturbance till the slope becomes infinity. According to Muralidharan and Sujith,¹⁷ the evolution of the leading edge of a finite-amplitude wave propagating in a stationary vapor in the presence of entropy gradients is

$$\frac{1}{u_1(x)} = \frac{F(0)}{F(x)u_1(0)} + \frac{1}{F(x)} \int_0^x \frac{F(\hat{x})\Gamma_0(\hat{x})}{c_0(\hat{x})} d\hat{x}, \quad (6)$$

where u is the particle velocity and

$$u_1(x) = \frac{d}{dx} [u(x)] \quad (7)$$

$$F(x) = c_0(x)^{-3/2} \rho_0(x)^{-1/2}, \quad \text{and} \quad x = X(t), \quad (8)$$

with $u_1(0)$ being the initial slope of the wave, $X(t)$ the location of the leading edge of the wave at time t , and c_0 and ρ_0 the local sound speed and density of the undisturbed medium. A shock is formed if $u_1(x) \rightarrow \infty$. The local rate of change of $1/u_1$, which is a measure of the curvature of the wavefront, can be derived from Eq. (6) and is written as

$$\frac{d}{dx} \left(\frac{1}{u_1} \right) = \frac{\Gamma}{c} - \frac{1}{u_1} \left[\frac{1}{F(x)} \frac{d}{dx} [F(x)] \right]. \quad (9)$$

This numerical method provides a closed-form solution which is at the foundation of the study on the effect of temperature variations on wave steepening. Equation (6) provides the wave slope only at the leading edge and, therefore, does not capture shocks formed elsewhere along the wave. This is, however, consistent with the current study, which also focuses on the steepening at the leading edge of the wave.

III. RESULTS

The wavefront expansion method was used to investigate the propagation of waves in the dense vapor of dodecamethylcyclohexasiloxane, D_6 , a complex organic molecule considered in recent theoretical, numerical, and experimental studies on nonclassical gasdynamics.²⁷ The properties of the fluid are computed using a Span–Wagner multiparameter equation of state model^{28,29} implemented in an in-house software library for the computation of fluid thermophysical properties.³⁰ Since the pressure of the medium is assumed constant, the variation of the temperature alone can completely describe the thermodynamic state of the fluid.

Moreover, the treatment is simplified by the adoption of the non-dimensional parameters,

$$x^* = x/L_0 \quad \text{and} \quad \eta = x - X(t),$$

where L_0 ($= 10$ m) and η are the domain length and the distance from the leading edge at time t , respectively.

A. Effect of temperature gradients on wave steepening

1. Uniform temperature

The effect of the variation of temperature, and therefore of Γ , on nonlinear wave propagation is first described in case a finite-amplitude wave travels in a fluid in which the temperature is homogeneous. In this case, Eq. (6) reduces to

$$\frac{1}{u_1} = \frac{1}{u_1(0)} + \Gamma_0 t, \tag{10}$$

where $\Gamma = \Gamma_0$ is the fundamental derivative evaluated for the thermodynamic state of the medium, which is, therefore, constant. The local rate of change of the wavefront slope $(1/u_1)'$ also simplifies to,

$$\frac{d}{dx} \left(\frac{1}{u_1} \right) = \frac{\Gamma_0}{c_0}. \tag{11}$$

Consequently, the sign and magnitude of Γ dictate the nature and rate of steepening of a nonlinear wave propagating in a constant-temperature medium. Equation (10) also shows that any traveling wave would necessarily undergo distortion, apart from the exceptional case of $\Gamma = 0$, entailing, therefore, linear propagation.

2. Non-uniform temperature

The effect of temperature variation within the fluid was investigated by means of simulations of the one-dimensional propagation of a rarefaction wave in the dense vapor of D_6 subjected to a linear temperature gradient, with temperatures varying from 369 °C to 373 °C over a length of 10 m and at an ambient pressure of 9 bar. These values were chosen because they are representative of nonclassical gasdynamic experiments by means of a shock tube documented in the literature and planned within this research project for the near future.⁹ However, the validity of the results does not depend on these values or fluid and a different fluid and similar reduced thermodynamic

properties would lead to similar results. The variation of Γ as a function of the non-dimensional tube length is shown in Fig. 1(a). For these fluid thermodynamic conditions, Γ transitions from negative values at lower temperature to positive values at higher temperature. It can, therefore, be expected that a rarefaction wave traveling in this medium would initially steepen for all locations within the tube in which Γ is negative and then relax further downstream.

This is indeed what is observed in Fig. 1(b), which shows the evolution of $1/u_1$ of rarefaction waves for different inverse initial slopes $1/u_1(0)$ resulting from calculations performed with the method illustrated in Sec. II C. The global trend for all rarefaction waves propagating in the fluid subjected to the temperature gradient shown in Fig. 1(a) is to initially steepen in portions of the flow domain in which the thermodynamic state features $\Gamma < 0$ followed by a relaxation in the portions featuring the $\Gamma > 0$ thermodynamic state. The value of $1/u_1$ reaches a minimum at the location where the steepening behavior of the wavefront reverses. As the initial strength of the wave increases (decreasing $1/u_1(0)$), this minimum value of $1/u_1$ gradually approaches zero until a shock is formed when $1/u_1 = 0$. The corresponding initial strength of the wave $\tilde{u}_1(0)$ is defined such that any wave with an initial slope larger than $\tilde{u}_1(0)$ can steepen to form a shock wave while a wave with $u_1(0) < \tilde{u}_1(0)$ cannot steepen sufficiently to form a shock wave in the medium.

Figure 1(b) shows also the line connecting the points of minimum of $1/u_1$ in the flow domain, denoted as $x_{\min\{1/u_1\}}$, for different $u_1(0)$ and where the thermodynamic state of the fluid features $\Gamma = 0$, denoted as $x_{\Gamma=0}$. In a fluid affected by temperature gradients, a rarefaction wavefront might be expected to steepen as long as the thermodynamic state implies that $\Gamma < 0$ and to relax if $\Gamma > 0$. The transition to the opposite steepening behavior of the wave would occur at the location where Γ is zero. However, as shown in Fig. 1(b), for all the initial wave strengths characterized by a value of the initial wave slope lower than $\tilde{u}_1(0)$, $x_{\min\{1/u_1\}}$ precedes $x_{\Gamma=0}$ along the x coordinate. Thus, the wave ceases to steepen and starts relaxing even if the

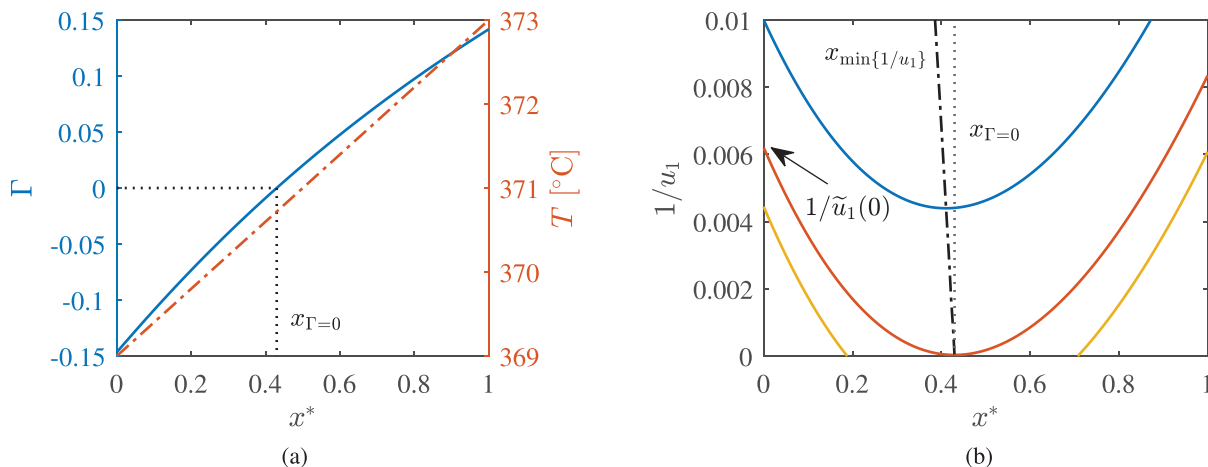


FIG. 1. Variation of relevant quantities as a function of the non-dimensional coordinate x^* related to the evolution of rarefaction waves in a one-dimensional flow domain ($x = 0 - 10$ m) formed by dense vapor of siloxane D_6 at $p = 9$ bar and subjected to a linearly increasing temperature change: (a) variation of T (Red dashed line) and Γ (Blue solid line), and (b) evolution of the inverse of the slope of the leading edge of rarefaction waves propagating along x^* , starting at $x^* = 0$ and $t = 0$ s with different values of $u_1(0)$. (---): locus of the positions in the flow domain where the wave features minimum $1/u_1$. (.....): locus of the positions in the flow domain for which the thermodynamic state of the fluid features $\Gamma = 0$.

thermodynamic state of the fluid features negative Γ . The value of Γ at the position where $x_{\min\{1/u_1\}}$ can be found from Eq. (9) as

$$\Gamma(x_{\min\{1/u_1\}}) = \frac{c}{u_1} \left[\frac{1}{F(x)} \frac{d}{dx} [F(x)] \right] \Big|_{x_{\min\{1/u_1\}}}. \quad (12)$$

Note that $F(x)$ defined in Eq. (8) has a finite value and dF/dx cannot be zero in a flow domain featuring gradients in fluid properties. Therefore, for Γ to be zero at $x_{\min\{1/u_1\}}$, $1/u_1$ must be necessarily zero at that location in a fluid subject to a temperature gradient indicating the formation of a shock wave. This leads to the definition of the critical initial slope condition $\tilde{u}_1(0)$.

The evolution of compression wavefronts propagating in a medium in which Γ changes from positive to negative was also studied. In this case, the temperature of the fluid decreases linearly from 373 °C to 369 °C. The variation of Γ and $1/u_1$ along the flow domain is shown in Figs. 2(a) and 2(b). Initially, the wave steepens as expected since $\Gamma > 0$, but the rate of steepening decreases as Γ approaches zero. Unlike the case of a medium subjected to a linearly increasing temperature, $x_{\min\{1/u_1\}}$ is greater than $x_{\Gamma=0}$ for all initial wave strengths $u_1(0) < \tilde{u}_1(0)$. Therefore, compression waves continue to steepen even if the local thermodynamic state of the fluid features negative Γ before starting to relax. Again, there exists a critical initial strength $\tilde{u}_1(0)$ for which $1/u_1$ is tangential to the x axis. This highlights the fact that the observed behavior is a general physical characteristic of nonlinear waves in the region close to $\Gamma = 0$ regardless of its sign.

3. Analysis based on the Westervelt equation

The propagation of finite-amplitude waves in a fluid affected by temperature variation is simulated by numerically solving the 1D Westervelt equation. Unlike the analytical solution of the one-dimensional wave propagation problem that can be derived from the 1D Euler equations, the Westervelt equation accounts for the

effect of viscosity. The effect of viscosity on wave propagation can be assessed by comparing the numerical solution of the Westervelt equation model to the analytical solution of the Euler equations.

Figure 3(a) shows the wavefront of a rarefaction wave, defined as a ramp in pressure and expressed in terms of acoustic velocity, at a given time instant while propagating in quiescent isothermal D_6 . The particle velocity increases linearly from $u = 0$ m/s at the wavefront ($\eta = 0$ m) till it reaches a maximum value of u_a at the tail of the wave, defined as

$$u_a = \frac{\Delta p}{\rho_0 \cdot c_0}, \quad (13)$$

where Δp is the pressure difference across the wave and ρ_0 and c_0 are the density and sound speed in the quiescent medium. Minor undulations can be observed along the wavefront, which result from the Gibb's oscillations forming at the two edges of the wavefront.

Figure 3(b) shows a closeup of the wavefront between the leading edge point ($\eta = 0$ m) and a location downstream of the wavefront. Though $1/u_1$ is calculated at the leading edge in the analytical solution, this does not yield accurate values in the simulation since it suffers from numerical dissipation at this location. This can be observed clearly at $\eta = 0$ m where the leading edge of the wavefront is smoothed due to dissipation. This has the tendency to artificially reduce the slope of the wavefront. To overcome this effect, the leading edge of the wavefront is reconstructed by calculating the actual leading edge location in the absence of numerical dissipation. This can be readily estimated owing to the fact that the leading edge is unaffected by nonlinear effects and propagates only at the local sound speed. Thus, the leading edge location at any time step n is

$$X(n) = X(n-1) + c(n-1) \cdot dt. \quad (14)$$

The slope between the leading edge point and a location at η along the wavefront is calculated as

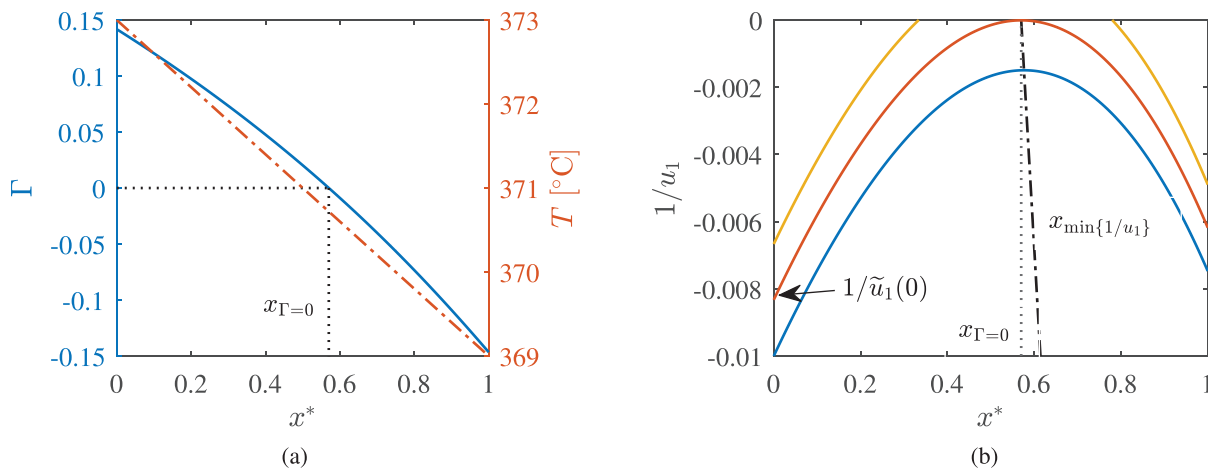


FIG. 2. Variation of relevant quantities as a function of the non-dimensional coordinate x^* related to the evolution of compression waves in a one-dimensional flow domain ($x = 0 - 10$ m) formed by dense vapor of siloxane D_6 at $p = 9$ bar and subjected to a linearly decreasing temperature change: (a) variation of T (Red dashed line) and Γ (Blue solid line), and (b) evolution of the inverse of the slope of the leading edge of rarefaction waves propagating along x^* , starting at $x^* = 0$ and $t = 0$ s with different values of $u_1(0)$. (---): locus of the positions in the flow domain where the wave features minimum $1/u_1$. (....): locus of the positions in the flow domain for which the thermodynamic state of the fluid features $\Gamma = 0$.

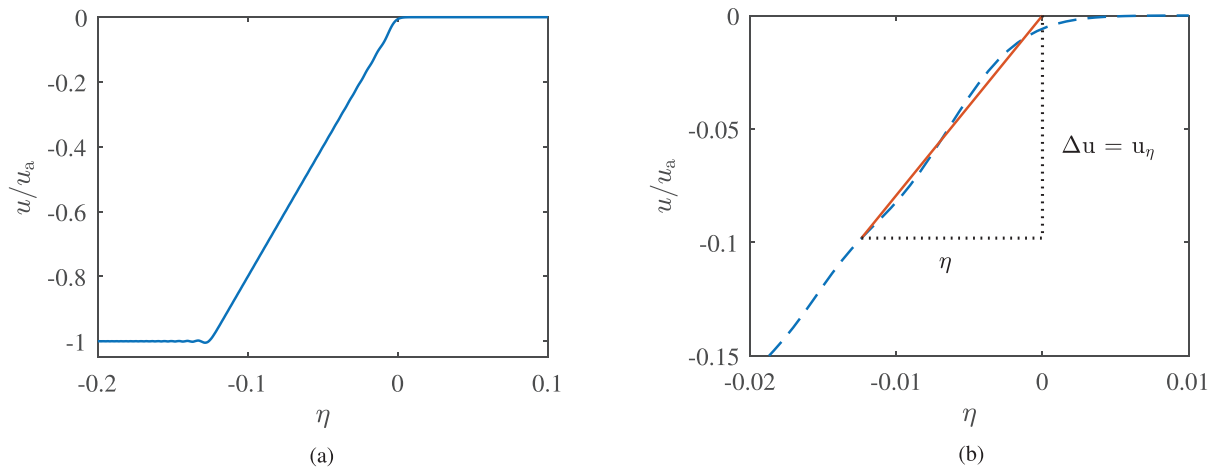


FIG. 3. (a) Variation in acoustic velocity as a function of $\eta = x - X(t)$ along the wavefront of a rarefaction wave propagating in dense vapor of isothermal D_6 at $p = 9$ bar and (b) closeup of the leading edge location showing the numerical dissipation and the method of estimation of the leading edge slope.

$$u_1|_{\text{numr.}} = \frac{u(\eta)}{\eta}. \tag{15}$$

The calculation of u_1 in this study is performed numerically at a location where $u(\eta) = 0.1u_a$. The sensitivity of u_1 to the choice of $u(\eta)$ was analyzed and was found to be small. Figure 4 compares the evolution of $1/u_1$ calculated using the analytical solution of the 1D Euler equations and the numerical solution of the Westervelt equation. As expected, both models predict a monotonous steepening of the wavefront until a shock wave is formed and the results are very similar, except for the fluctuations affecting the solution of the Westervelt equation arising from the Gibb's oscillations shown in Fig. 3(a).

Figure 5(a) shows the variation in the particle velocity along the wavefront at three different time instances for a rarefaction wave propagating in the dense vapor of D_6 subjected to linearly increasing temperature as shown in Fig. 1(a). The profile of the wavefront during the initial stage of propagation in the medium is shown for $t = 0.005$ s.

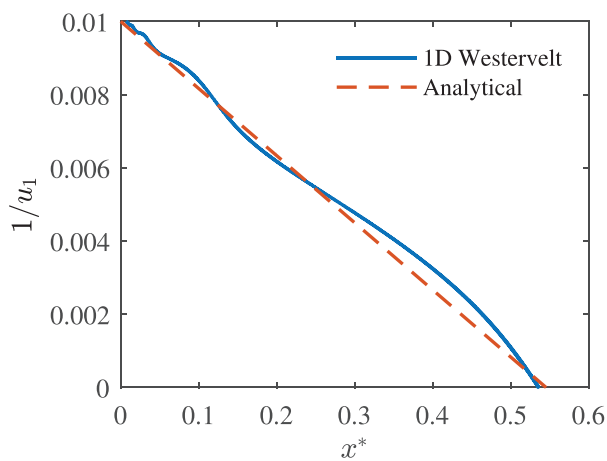


FIG. 4. Evolution of the inverse of the wavefront slope in isothermal D_6 at $p = 9$ bar propagating along x^* , starting at $x^* = 0$ and $t = 0$ s calculated using the analytical solution of the Euler equations and the solution of the Westervelt equation.

The particle velocity varies linearly from $u = 0$ at the leading edge to $u = u_a$ at the tail of the wave and the wavefront is largely devoid of any numerical oscillation. Since $\Gamma < 0$ in the fluid in this thermodynamic state, the wave steepens as it propagates. This steepening can be observed in the wavefront profile shown at $t = 0.1$ s. It is seen that the tail of the wave at this time instant lies closer to $\eta = 0$ m than at $t = 0.005$ s. At this time instant, the wave is close to the location of $x_{\min\{1/u_1\}}$ in Fig. 1(b). After this time, the fluid thermodynamic state features $\Gamma > 0$ and thus the wave relaxes during propagation. This is seen at $t = 0.15$ s in Fig. 5(a). Once again, the tail of the wave moves farther from $\eta = 0$ m, indicating that the wave is relaxing as it travels in the medium.

Another observation that can be deduced from Fig. 5(a) is related to the magnitude of u at the tail of the wave. Since the wave travels in a medium in which the temperature varies, the acoustic impedance z of the medium also varies with location. This results in a continuous reflection of a part of the incident wave in the upstream direction. Thus, the particle velocity at the tail end of the wave is higher than u_a as the wave progresses and increases steadily from $t = 0.005$ s to $t = 0.15$ s.

Figure 5(b) shows the evolution of $1/u_1$ calculated using both the analytical solutions to the 1D Euler equation and the Westervelt equation. The steepening of the wavefront computed using the Westervelt equation is seen to match closely with the analytical solution and captures the behavior accurately. Once again, numerical oscillations seen in Fig. 5(a) affect $1/u_1$ and the numerical slope fluctuates about the analytical solution.

It can, therefore, be concluded that the variation of temperature significantly affects the steepening characteristics of finite-amplitude waves propagating in dense vapors of fluids made of complex molecules. If the fluid is in a thermodynamic state close to states for which $\Gamma = 0$, the effect of sound speed and density variation can alter the steepening of the wave in a way that is opposite to that dictated by the local value of Γ . Unless the wave features a critical initial strength $\tilde{u}_1(0)$, then it is shown that a rarefaction wave can relax even if it propagates through a fluid for which the thermodynamic state features $\Gamma < 0$ and vice versa for a compression wave.

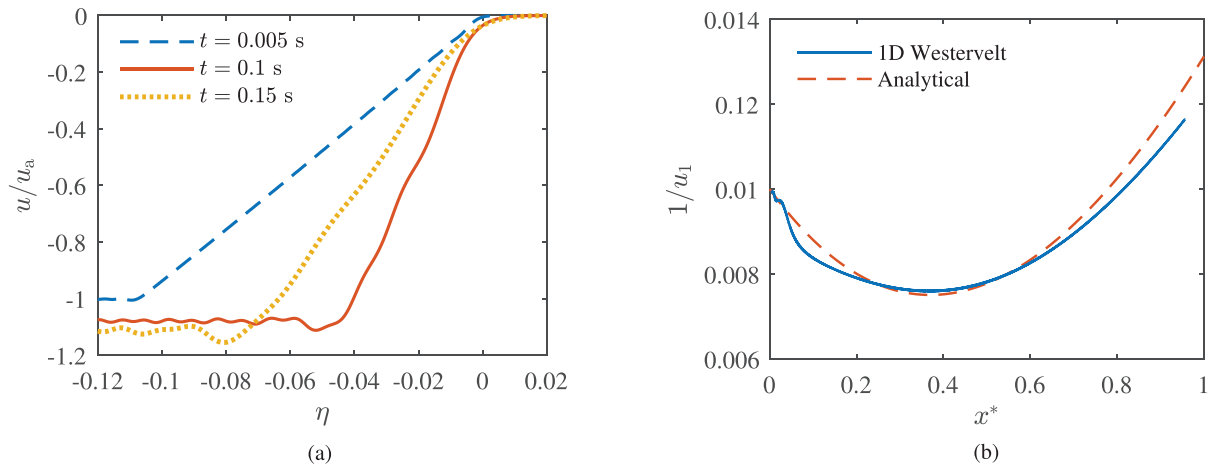


FIG. 5. (a) Particle velocity u vs η ($= x - X(t)$) along a rarefaction wave propagating in D_6 subjected to linearly increasing temperature at three different time instances and (b) comparison of evolution of $1/u_1$ between the analytical solution to 1D Euler equations and the solution of the Westervelt equation.

In addition, numerical simulations of wave propagation show that viscosity has a negligible effect on wave steepening even if the wave propagates in a fluid whose thermodynamic state features Γ close to zero.

B. Effect of temperature gradients on shock formation

Apart from the scientific interest of understanding how temperature variations influence the propagation of waves in dense vapors, the results of this investigation are of particular relevance regarding experiments aimed at generating and proving the formation of a rarefaction shock with a shock tube experiment. In such an experiment, one is interested in obtaining the shortest shock formation distance to keep the length of the shock tube as short as possible.

As an example relevant to the experimental study of nonclassical gasdynamics, the propagation of a rarefaction wave in a tube containing dense vapor of siloxane D_6 and subjected to a sinusoidal fluctuation of temperature around a mean value along its length was numerically investigated. This type of temperature perturbation allows to study the effect of both the amplitude and wavelength of the disturbance on wave evolution. The temperature perturbation is, therefore,

$$T = T_0 + \Delta T \cdot \sin\left(\frac{2\pi x}{\lambda_T} + \phi\right), \quad (16)$$

where T_0 is the temperature of the quiescent fluid in $^\circ\text{C}$, ΔT is the amplitude of temperature variation in $^\circ\text{C}$, λ_T is the wavelength of the temperature variation in meters, and $\phi \in [-\pi, \pi]$ is the phase of the sinusoidal disturbance. The evolution of the wavefront is analyzed for M values of λ_T and N values of ϕ , linearly distributed over their range and indexed as $\lambda_{T,i}$ ($i = 1, 2, \dots, M$) and ϕ_j ($j = 1, 2, \dots, N$), and the corresponding shock formation distances x_{sh} are calculated. To remove the effect of the initial phase of the disturbance, mean shock distances \bar{x}_{sh} rather than a single shock distance x_{sh} dependent on the initial phase are compared. The mean shock distances are, therefore, computed as

$$\bar{x}_{sh}(i) = \frac{\sum_{j=1}^N x_{sh}(\lambda_{T,i}, \phi_j)}{N}, \quad (17)$$

and are compared with the shock distance $x_{sh,homog}$ that is computed for the case in which the properties of the medium are homogeneous, with temperature equal to the mean temperature of the sinusoidal profile. The non-dimensional parameters,

$$\lambda^* = \lambda_T/L_0, \quad x^* = x/L_0,$$

and

$$x_{sh}^* = x_{sh}/x_{sh,homog}, \quad \bar{x}_{sh}^* = \bar{x}_{sh}/x_{sh,homog},$$

facilitate the analysis of the results. In these definitions, L_0 ($=10$ m) and $x_{sh,homog}$ are the fluid domain length and the shock formation distance in a homogeneous fluid, respectively.

1. Rarefaction waves

The fluid thermodynamic state chosen for this analysis is such that $\Gamma < 0$ everywhere in the domain. Rarefaction waves with different initial wave slopes $u_1(0)$ were simulated to propagate in dense vapor of D_6 at 9 bar and subjected to a sinusoidal temperature disturbance defined by Eq. (16) with $T = 369$ $^\circ\text{C}$, $\Delta T = 0.5$ $^\circ\text{C}$, $M = 10$ and $N = 200$. In this thermodynamic state, the mean value of Γ is -0.14 .

Figure 6 shows the variation of the mean shock formation distance \bar{x}_{sh}^* as a function of λ^* for pressure waves with different values of $u_1(0)$. Figure 6(a) highlights that \bar{x}_{sh}^* is between 0.96 and 0.99 for $\lambda^* \leq 0.1$ for all values of $u_1(0)$. This implies that the shock formation distance is only weakly dependent on the initial wave slope for $\lambda^* < 0.1$. It can also be observed that, though $\bar{x}_{sh}^* < 1$, the spread in the mean shock distance increases with increasing λ^* . Figure 6(b) puts into evidence that, for $\lambda^* > 0.1$, the mean shock formation distance increases with increasing λ^* , eventually reaching a value greater than 1. Also, the variation of \bar{x}_{sh}^* with λ^* exhibits a stronger dependency on

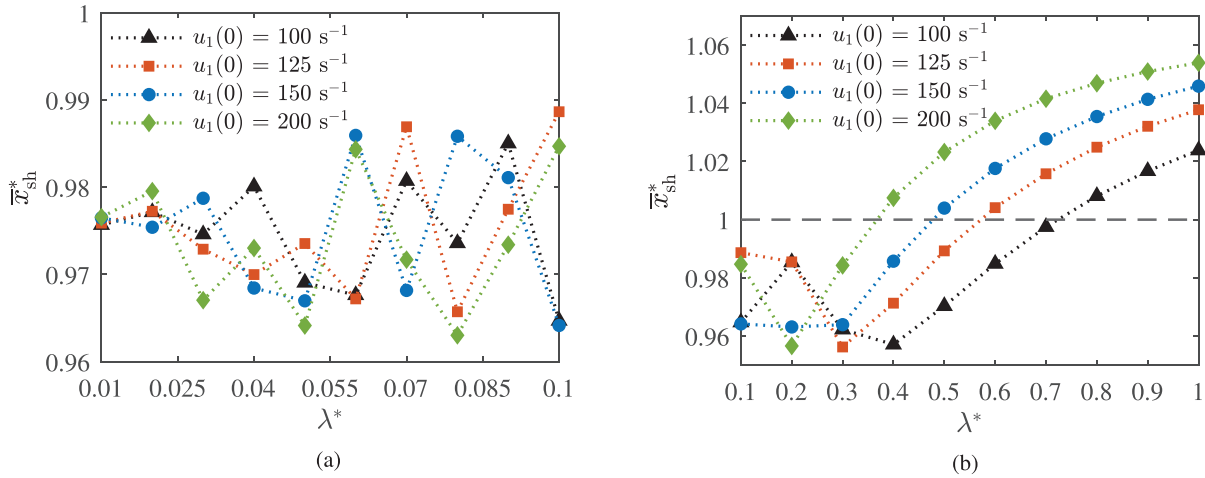


FIG. 6. Variation of \bar{x}_{sh} as a function of λ^* for rarefaction waves with different values of initial slope $u_1(0)$ evolving in dense vapors of D_6 at $p = 9$ bar and subjected to a sinusoidally varying temperature: (a) $\lambda^* < 0.1$ and (b) λ^* between 0.1 and 1.

$u_1(0)$: as the initial slope of the wave increases, the minimum wavelength at which \bar{x}_{sh}^* starts increasing toward 1 decreases.

Figure 7 compares the evolution of $1/u_1$ in a fluid affected by a sinusoidal temperature variation with $\lambda^* = 0.05$ and $\phi = \pi/2$ with the evolution of $1/u_1$ for a wave that propagates in a homogeneous medium. The choice of the values of λ^* and ϕ was made to highlight the effect of the temperature gradient on wave evolution and has no impact on the previous observations. Similarly to what is displayed in Figs. 1(b) and 2(b), the rarefaction wave steepens if the fluid is in a thermodynamic state featuring negative Γ and relaxes if $\Gamma > 0$. The undulations in the slope of the evolving wavefront in Fig. 7(a) are caused by the periodic oscillation of the local temperature, and therefore of Γ . It can be seen in Fig. 7(b), which is a close-up of Fig. 7(a) and shows the early evolution of the wave, that the steepening phase of

the wave is more prominent than the relaxing phase. This observation can be explained by means of Eq. (9), rewritten here for better clarity, as

$$\frac{d}{dx} \left(\frac{1}{u_1} \right) = \frac{\Gamma}{c} - \frac{\kappa}{u_1}, \tag{18}$$

where

$$\kappa \equiv \left[\frac{1}{F(x)} \frac{d}{dx} [F(x)] \right],$$

which shows that $(1/u_1)'$ depends on both the local values of Γ and c as well as on the gradient of sound speed and density.

Figure 8 displays the variation of the two terms constituting Eq. (18) for two different values of λ^* . The first term, Γ/c , is directly

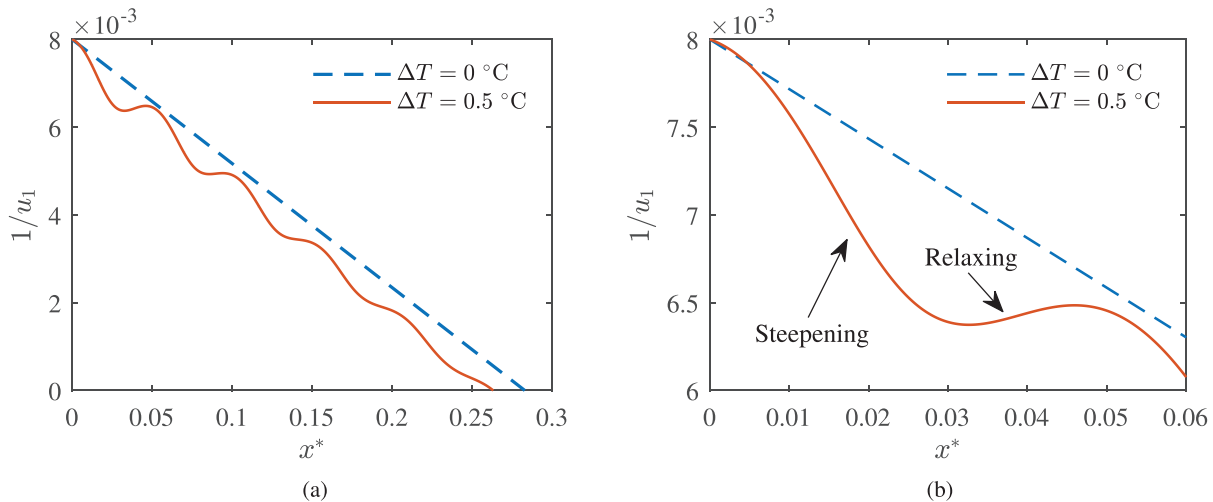


FIG. 7. Variation of relevant quantities as a function of the non-dimensional coordinate x^* related to the evolution of rarefaction waves in a one-dimensional flow domain ($x = 0 - 10$ m) formed by dense vapor of siloxane D_6 at $p = 9$ bar and subjected to a sinusoidal temperature change [see Eq. (16)] with $\lambda^* = 0.05$ and $\phi = \pi/2$: (a) evolution of $1/u_1$ of the rarefaction wave propagating along x^* , starting at $x^* = 0$ and $t = 0$ s, till $x^* = x_{sh}^*$, and (b) closeup of evolution of $1/u_1$ from $x^* = 0 - 0.06$ for better clarity.

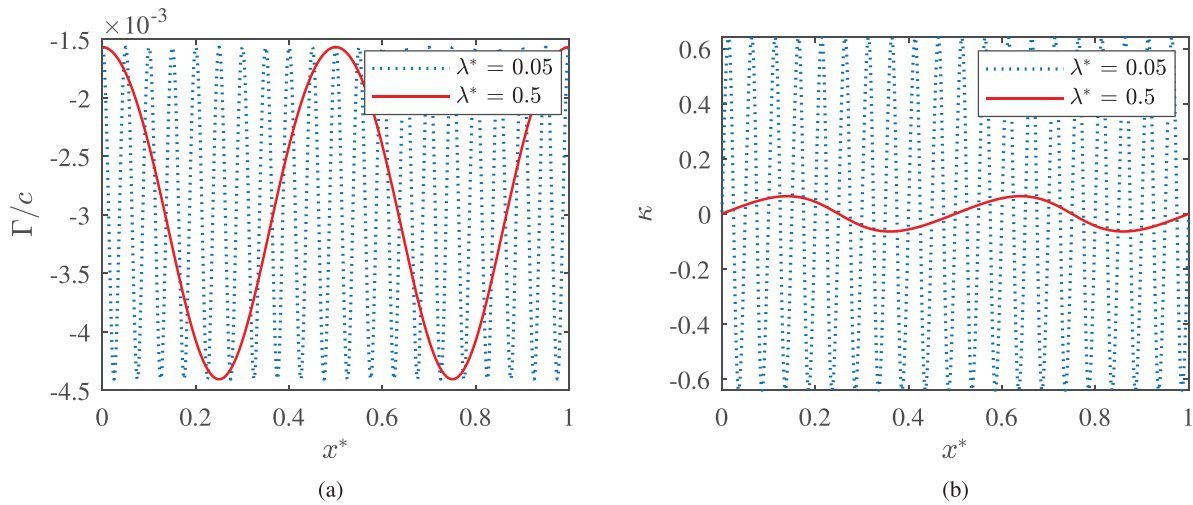


FIG. 8. Variation of relevant quantities constituting Eq. (18) as a function of the non-dimensional coordinate x^* in dense vapor of siloxane D_6 at $p = 9$ bar and subjected to a sinusoidal temperature change with $\Delta T = 0.5$ °C and for $\lambda^* = 0.05$ and 0.5 : (a) variation of Γ/c and (b) variation of κ .

determined by the local temperature in the medium and, therefore, shows a similar sinusoidal oscillation. Since the fluid is in a state in which $\Gamma < 0$, this term is negative everywhere in the fluid. The second term, κ/u_1 , is also determined by the initial conditions of the medium. However, κ can either be positive or negative depending on whether the location is on the increasing or the decreasing branch of the sinusoidal temperature gradient. If $\kappa < 0$, the cumulative effect of the negative contributions of both terms enhances the nonclassical steepening of the rarefaction wave. However, if κ is positive, the contributions have opposite sign and the relaxing of the wave is mitigated. This explains why a shorter shock formation distance is calculated in a wave propagating through a medium with temperature gradients when compared to a medium with homogeneous temperature distribution.

In Eq. (18), κ is modulated by the local inverse slope of the wavefront $1/u_1$; therefore, the magnitude of κ/u_1 reduces as the wave steepens ($1/u_1 \rightarrow 0$) to form a shock. Since the magnitude of Γ/c is smaller than κ/u_1 (see Fig. 8), the undulations are dampened as the wave steepens during propagation, as seen in Fig. 7. Figure 8 also highlights the effect of the change in the wavelength of the temperature distribution on Γ/c and κ/u_1 . As the wavelength increases, the magnitude of Γ/c remains constant but the value of κ decreases significantly owing to the smaller gradients in sound speed and density in a fluid whose temperature varies less sharply. Thus, at higher λ^* , the enhancement of nonlinear steepening caused by κ decreases. This also explains the inverse dependence among x_{sh}^* and $u_1(0)$ for $\lambda^* > 0.1$: the contribution of κ/u_1 , which is already lower at higher λ^* , is further reduced due to smaller $1/u_1$ (higher $u_1(0)$) leading to the behavior observed in Fig. 6(b).

Figure 9 shows the variation of the shock formation distance x_{sh}^* as a function of ϕ for λ^* equal to 0.05 and to 0.5 for two initial wave slopes of 100 and 200 s^{-1} . The enhancement of the nonlinear steepening of the wave by the gradients in sound speed and density can be observed in the lines showing the variation of x_s^* with ϕ for $\lambda^* = 0.05$. For both cases of $u_1(0)$, the variation of x_{sh}^* with λ^* is similar and

superimpose each other highlighting the independence of x_{sh}^* from $u_1(0)$ as observed in Fig. 6(a). Also, x_{sh}^* is close to 1 or lower than 1 for both $u_1(0)$, indicating that the gradients in sound speed and density ensure that the wave in this medium almost always shocks earlier than in a homogeneous medium. For $\lambda^* = 0.5$, the variation in x_s^* with ϕ is more significant due to the smaller gradients in sound speed and density associated with this temperature variation. For both the initial wave slope cases, x_s^* is greater than 1 for certain ϕ . This effect is stronger for $u_1(0) = 200 s^{-1}$ where, in addition to the smaller value of κ , the contribution of the κ/u_1 term in Eq. (18) is also smaller owing to the lower value of $1/u_1(0)$. Thus, the shock formation distance is more susceptible to the phase of the sinusoidal temperature distribution as the wavelength of this variation increases.

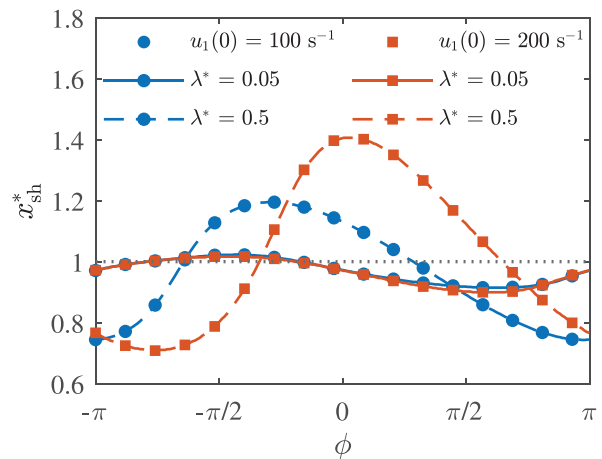


FIG. 9. Variation of shock formation distance x_{sh}^* as a function of the phase of the sinusoidal temperature gradient ϕ for rarefaction waves with different $u_1(0)$ evolving in dense vapor of D_6 at $p = 9$ bar and subjected to a temperature distribution given by Eq. (16) for different λ^* .

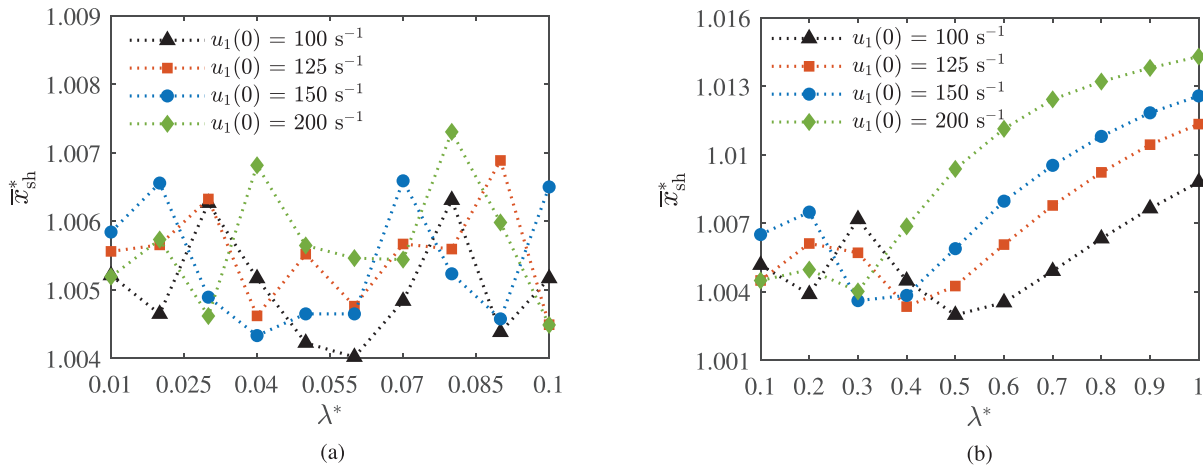


FIG. 10. Variation of \bar{x}_{sh}^* as a function of λ^* for compression waves with different values of initial slope $u_1(0)$ evolving in dense vapors of D_6 at $p = 9$ bar and subjected to a sinusoidally varying temperature: (a) $\lambda^* < 0.1$ and (b) λ^* between 0.1 and 1.

The results presented here indicate that, contrary to the intuition that a temperature gradient in an experimental setup aimed at generating a rarefaction shock wave would be detrimental with respect to nonlinear steepening, a temperature variation can help enhance the steepening of a propagating finite-amplitude wave and can in fact cause the wave to steepen into a shock at a shorter distance from the wave origin if compared to the wave propagation in a homogeneous medium. This outcome has a significant impact on rarefaction shock wave experiments using shock tubes, because inevitable fluctuations of the temperature along the tube can be controlled to cause a shorter shock formation distance. The results also show that the shock formation distance is the lowest when the wave initially encounters a $\Gamma < 0$ region during propagation in an inhomogeneous fluid. Thus, even in experiments without inherent temperature gradients, or in situations where maintaining one across the setup is not feasible, the shock formation distance can be reduced by simply altering the conditions in the region close to the wave origin to obtain a value of Γ that is lower than elsewhere.

2. Compression waves

The fluid thermodynamic state chosen for this analysis is such that $\Gamma > 0$ everywhere in the fluid domain. Compression waves with different initial waveslopes $u_1(0)$ were simulated to propagate in dense vapor of D_6 at 9 bar and subjected to a sinusoidal temperature disturbance defined by Eq. (16) with $T = 373^\circ C$, $\Delta T = 0.5^\circ C$, $M = 10$, and $N = 200$. In this thermodynamic state, the mean value of Γ is 0.11.

Figure 10 shows the variation in mean shock formation distance \bar{x}_{sh}^* for different λ^* . It is seen that for all λ^* , the mean shock distance is greater than the homogeneous shock formation distance $x_{sh,homog}$. The variation of \bar{x}_{sh}^* with λ^* , however, is similar to what can be observed in Fig. 6, wherein \bar{x}_{sh}^* remains fairly constant for $\lambda^* < 0.1$ and then increases depending on $u_1(0)$ for $\lambda^* > 0.1$. It can also be noticed that the variations in \bar{x}_{sh}^* in this case are not more than 1.5% in the considered range of λ^* , which is significantly lower than the observed variations in \bar{x}_{sh}^* seen in Fig. 6.

Figure 11 shows the comparison of the evolution of the compression wavefront in a fluid affected by sinusoidal temperature variation with $\lambda^* = 0.05$ and $\phi = \pi/2$ with the evolution of $1/u_1$ for a wave that propagates in a homogeneous medium. Unlike what can be seen in Fig. 7, the rate of steepening of the wavefront is nearly constant with only minor undulations. For this combination of ϕ and λ^* , the shock formation distance in the fluid affected temperature gradients is only marginally smaller than that in the fluid subjected to uniform temperature. Similar to what is observed in Fig. 7(a), the undulations in the evolution of $1/u_1$ are dampened in this case also as the wave approaches shock formation.

The reason for the dampened response of $1/u_1$ to the variation in Γ and κ can be attributed to the lower sensitivity of Γ , ρ & c to temperature variations in this thermodynamic region. Figure 12 depicts

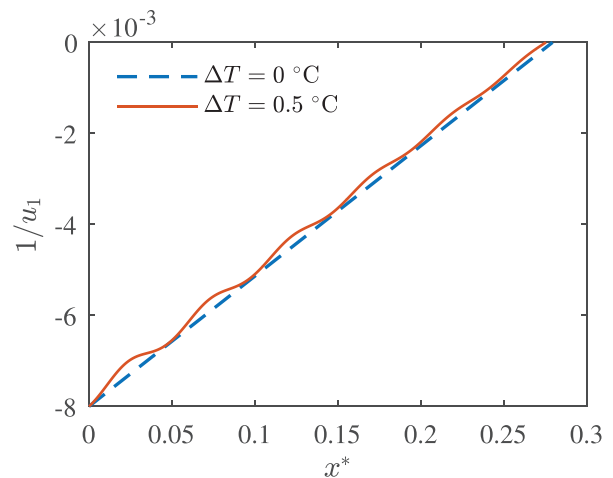


FIG. 11. Evolution of $1/u_1$ of a compression wave propagating along x^* , starting at $x^* = 0$ and $t = 0$ s, till $x^* = x_{sh}^*$ in a one-dimensional flow domain ($x = 0 - 10$ m) formed by dense vapor of siloxane D_6 at $p = 9$ bar and subjected to a sinusoidal temperature change [see Eq. (16)] with $\lambda^* = 0.05$ and $\phi = \pi/2$.

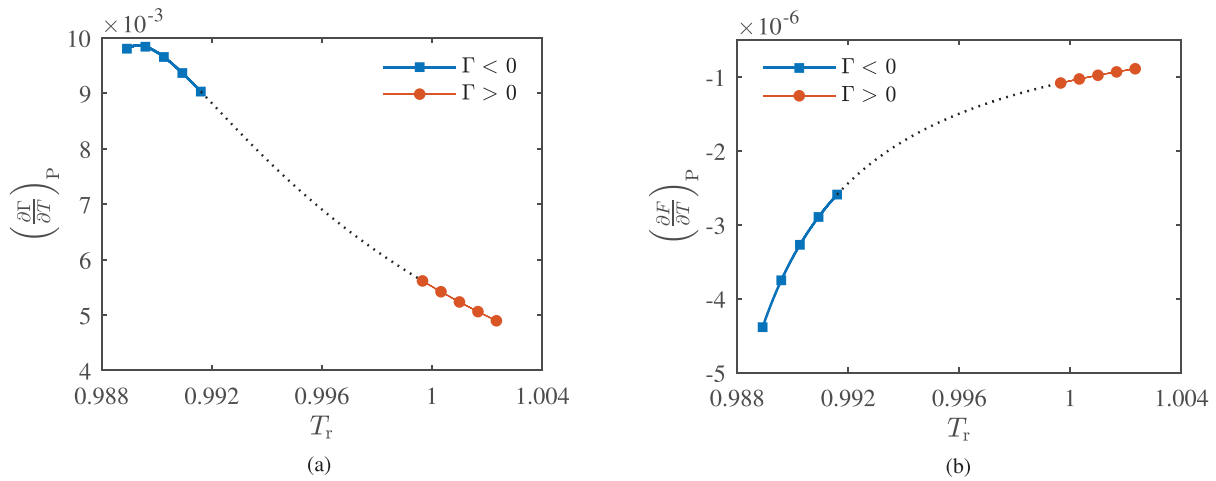


FIG. 12. Variation in (a) $(\frac{\partial \Gamma}{\partial T})_P$ and (b) $(\frac{\partial F}{\partial T})_P$ vs T_r along the isobar $P_r = 0.94$. Values of the gradients in the range of temperatures observed in Figs. 6 and 10 in the $\Gamma < 0$ and $\Gamma > 0$ thermodynamic regions are highlighted.

the variation in $(\partial \Gamma / \partial T)_P$ and $(\partial F / \partial T)_P$ with the reduced temperature T_r along the isotherm at $P_r = 0.94$ in the range of temperatures related to the cases presented in Secs. III B 1 and III B 2, in the $\Gamma < 0$ and $\Gamma > 0$ domains. It is seen that the gradients in Γ are approximately twice as large in $\Gamma < 0$ region [Fig. 12(a)], while the gradients in F are three times larger in the same regime [see Fig. 12(b)] when compared to those in the $\Gamma > 0$ region. Thus, the impacts of the variations in medium properties on $(1/u_1)'$ and $(1/u_1)$ are much smaller in the $\Gamma > 0$ region when compared with those in the $\Gamma < 0$ region. This results in a smaller perturbation of the propagating wave, resulting in similar or longer shock formation distances than those calculated for the case of homogeneous medium.

IV. CONCLUSIONS

This article presents the results of an analytical and numerical investigation on the effect of axial temperature gradients on the propagation of finite amplitude waves in the dense vapor of BZT fluids, therefore, in the case of nonclassical gasdynamics. The evolution and the steepening of the wavefront were studied analytically by means of a closed-form solution of the one-dimensional governing equation. A model based on the Westervelt equation was developed in order to simulate wave propagation and visualize simulation results. The analysis was performed by assuming that the dense vapor is that of siloxane D_6 , initially isobaric conditions. Different temperature variations along the physical domain were considered.

The model allowed us to demonstrate analytically that, if the wave propagates nonclassically, there exists a minimum initial value of the slope of a finite-amplitude wave, which allows the wave to steepen into a shock, if the fluid is subjected to a variation of temperature along the flow domain. While Γ determines the nature of the steepening of propagating disturbances for the most part, there exists a small region close to $\Gamma = 0$ in which the gradients in sound speed and density overcome the effect of nonlinearity on the distortion of the wave. If the state of the fluid lies in this thermodynamic region, a rarefaction wave can relax even if $\Gamma < 0$, and a compression wave can steepen even if $\Gamma > 0$.

The effect of gradients in sound speed and density are also shown to significantly influence the location of the shock formation. The results show that rarefaction waves evolving in a fluid for which $\Gamma < 0$ and subjected to temperature gradients tend to shock at a shorter distance from the wave origin if compared to the case in which the fluid is at uniform temperature. Furthermore, this effect of enhanced non-linear steepening is shown to decrease with increasing initial wave slopes. Compression waves evolving in a fluid for which $\Gamma > 0$ are seen to be less influenced by the gradients of the medium properties owing to the lower sensitivity of these properties to temperature variations in this thermodynamic region.

ACKNOWLEDGMENTS

This research has been supported by the Engineering Sciences Division (TTW) of the Dutch Organization for Scientific Research (NWO), Technology Program of the Ministry of Economic Affairs, Grant No. 15837.

AUTHOR DECLARATIONS

Conflict of Interest

The authors have no conflicts of interest to disclose.

DATA AVAILABILITY

The data that support the findings of this study are available from the corresponding author upon reasonable request.

REFERENCES

- ¹P. A. Thompson, "A fundamental derivative in gasdynamics," *Phys. Fluids* **14**, 1843–1849 (1971).
- ²A. Kluwick, "Chapter 3.4—Rarefaction shocks," in *Handbook of Shock Waves*, edited by G. Ben-Dor, O. Igra, and T. Elperin (Academic Press, Burlington, 2001), pp. 339–411.
- ³A. Kluwick, "Non-ideal compressible fluid dynamics: A challenge for theory," *J. Phys.: Conf. Ser.* **821**, 012001 (2017).
- ⁴C. Zamfirescu, A. Guardone, and P. Colonna, "Admissibility region for rarefaction shock waves in dense gases," *J. Fluid Mech.* **599**, 363–381 (2008).

- ⁵A. A. Borisov, A. A. Borisov, S. S. Kutateladze, and V. E. Nakoryakov, "Rarefaction shock wave near the critical liquid-vapour point," *J. Fluid Mech.* **126**, 59–73 (1983).
- ⁶N. R. Nannan, A. Guardone, and P. Colonna, "On the fundamental derivative of gas dynamics in the vapor-liquid critical region of single-component typical fluids," *Fluid Phase Equilib.* **337**, 259–273 (2013).
- ⁷S. Ferguson, A. Guardone, and B. Argrow, "Construction and validation of a dense gas shock tube," *J. Thermophys. Heat Transfer* **17**, 326–333 (2003).
- ⁸L. Calderazzi and P. Colonna, "Thermal stability of R-134a, R-141b, R-131i, R-7146, R-125 associated with stainless steel as a containing material," *Int. J. Refrig.* **20**, 381–389 (1997).
- ⁹T. Mathijssen, M. Gallo, E. Casati, N. R. Nannan, C. Zamfirescu, A. Guardone, and P. Colonna, "The flexible asymmetric shock tube (FAST)—A Ludwig tube facility for wave propagation measurements in high-temperature vapours of organic fluids," *Exp. Fluids* **56**, 195 (2015).
- ¹⁰P. Colonna, A. Guardone, N. R. Nannan, and C. Zamfirescu, "Design of the dense gas flexible asymmetric shock tube," *J. Fluid Eng.-Trans. ASME* **130**, 034501 (2008).
- ¹¹P. Colonna and P. Silva, "Dense gas thermodynamic properties of single and multi-component fluids for fluid dynamics simulations," *J. Fluid Eng.-Trans. ASME* **125**, 414–427 (2003).
- ¹²C. Zamfirescu, A. Guardone, and P. Colonna, "Preliminary design of the FAST dense gas Ludwig tube," AIAA Paper No. 2006-3249, 5–8 June, 2006.
- ¹³V. S. Soukhomlinov, V. Y. Kolosv, V. A. Sheverev, and M. V. Ötügen, "Formation and propagation of a shock wave in a gas with temperature gradients," *J. Fluid Mech.* **473**, 245–264 (2002).
- ¹⁴H. Lin and A. J. Szeri, "Shock formation in the presence of entropy gradients," *J. Fluid Mech.* **431**, 161–188 (2001).
- ¹⁵M. S. Cramer and A. Kluwick, "On the propagation of waves exhibiting both positive and negative nonlinearity," *J. Fluid Mech.* **142**, 9–37 (1984).
- ¹⁶M. S. Cramer and R. Sen, "Shock formation in fluids having embedded regions of negative nonlinearity," *Phys. Fluids* **29**, 2181–2191 (1986).
- ¹⁷S. Muralidharan and R. I. Sujith, "Shock formation in the presence of entropy gradients in fluids exhibiting mixed nonlinearity," *Phys. Fluids* **16**, 4121–4128 (2004).
- ¹⁸P. Jordan, R. Keiffer, and G. Saccomandi, "A re-examination of weakly-nonlinear acoustic traveling waves in thermoviscous fluids under Rubin-Rosenau-gottlieb theory," *Wave Motion* **76**, 1–8 (2018).
- ¹⁹P. Colonna, N. R. Nannan, A. Guardone, and E. W. Lemmon, "Multiparameter equations of state for selected siloxanes," *Fluid Phase Equilib.* **244**, 193–211 (2006).
- ²⁰I. Shevchenko and B. Kaltenbacher, "Absorbing boundary conditions for non-linear acoustics: The Westervelt equation," *J. Comput. Phys.* **302**, 200–221 (2015).
- ²¹G. F. Pinton, J. Dahl, S. Rosenzweig, and G. E. Trahey, "A heterogeneous non-linear attenuating full-wave model of ultrasound," *IEEE Trans. Ultrason., Ferroelectr., Frequency Control* **56**, 474–488 (2009).
- ²²Y. Jing, T. Wang, and G. T. Clement, "A k-space method for moderately non-linear wave propagation," *IEEE Trans. Ultrason., Ferroelectr., Frequency Control* **59**, 1664–1673 (2012).
- ²³M. F. Hamilton, D. T. Blackstock *et al.*, *Nonlinear Acoustics* (Academic Press, San Diego, 1998), Vol. 237.
- ²⁴W. Lauterborn, T. Kurz, and I. Akhatov, *Nonlinear Acoustics in Fluids*, Springer Handbook of Acoustics (Springer, New York, 2014), pp. 265–314.
- ²⁵R. T. Beyer, "Parameter of nonlinearity in fluids," *J. Acoust. Soc. Am.* **32**, 719–721 (1960).
- ²⁶A. A. Haigh, B. E. Treeby, and E. C. McCreath, "Ultrasound simulation on the cell broadband engine using the westervelt equation," in *Proceedings of the 12th International Conference on Algorithms and Architectures for Parallel Processing—Volume Part I, ICA3PP'12* (Springer-Verlag, Berlin, Heidelberg, 2012), pp. 241–252.
- ²⁷P. Colonna, A. Guardone, and N. R. Nannan, "Siloxanes: A new class of candidate Bethe-Zel'dovich-Thompson fluids," *Phys. Fluids* **19**, 086102–086112 (2007).
- ²⁸P. Colonna, N. R. Nannan, and A. Guardone, "Multiparameter equations of state for siloxanes: $[(\text{CH}_3)_3\text{Si-O}^{1/2}]_2\text{-[O-Si-(CH}_3)_2]^{1-1.3}$, and $[\text{O-Si-(CH}_3)_2]_6$," *Fluid Phase Equilib.* **263**, 115–130 (2008).
- ²⁹R. Span, *Multiparameter Equations of State* (Springer Berlin Heidelberg, 2000).
- ³⁰P. Colonna, T. P. van der Stelt, and A. Guardone, "FluidProp (Version 3.1): A program for the estimation of thermophysical properties of fluids a computer program since 2004," a computer program since 2004 (2019), see <http://www.asimptote.nl/software/fluidprop>.